Clays and Clay Minerals, Vol. 44, No. 4, 501–505, 1996.

INTERCALATION OF N-ALKYLTRIMETHYLAMMONIUM INTO SWELLING FLUORO-MICA

KENJI TAMURA[1] AND HIROMOTO NAKAZAWA[2]

[1] Kawasaki Plastics Laboratory, Showa Denko K.K., 3-2 Chidori-cho, Kawasaki-ku, Kawasaki, Kanagawa, 210 Japan

[2] National Institute for Research in Inorganic Materials, 1-1 Namiki, Tsukuba, Ibaraki, 305 Japan

Abstract—Trimethylammonium ions (TMA^+) with formula $CH_3(CH_2)_{n-1}N^+(CH_3)_3$, with n = 4, 8, 12, 16, 18 and 22 were intercalated into synthetic Li-fluorotaeniolite (Li-FTN) and Li-fluorohectorite (Li-FHT) by cation exchange. The products were analyzed by thermogravimetric (TGA) and X-ray powder diffraction (XRD). XRD patterns exhibited variable (001) spacings of the TMA^+/mica complexes depending upon the exchange ratio of TMA^+/Li^+ and the carbon number of TMA^+. Detailed inspection of these XRD patterns clarified the structures of the complexes and also the intercalation mechanism, as follows: The fundamental structure of the complexes is the commonly known intercalation structure where the "paraffin-type bilayers" of TMA^+ are in the mica interlayer and their long chains incline at approximately 30° to the silicate sheet. This structure appeared at the final stage of the intercalation reaction. During the intermediate stage of the reaction, units of this structure and those of hydrated mica formed randomly and regularly interstratified structures. Variable (001) spacings in XRD patterns showed the structural change of the complex with an increasing number of TMA^+-intercalated units.

Key Words—Fluoro-Mica, Intercalation, N-Alkyltrimethylammonium, XRD Cation Exchange.

INTRODUCTION

Organo-clay complexes have found applications for various fields. For example, reinforced plastics (Fukushima and Inagaki 1987; Messersmith and Giannelis 1994; Wang and Pinnavaia 1994), rheological control agents (Magauran et al. 1987) and chemical sensors (Yan and Bein 1993). Their properties depend upon the properties of the intercalated organic molecules but also strongly upon the physiochemical nature of the host crystals. These studies used natural clays as host crystals and investigated the structure of the complexes (Lagaly and Weiss 1969), adsorption of organic molecules (Farmar and Mortland 1965) and others. However, the natural clays have properties that must be interpreted as a result of inhomogeneous inter- and intra-charge distribution and impurity of materials. A clay mineralogy text book describes the inhomogeneous nature as "the rule with natural montmorillonite" (MacEwan and Wilson 1980). The uncontrollable nature of natural clays gives effect of the broad characteristics of organo-clay complexes.

Recently, fluoro-micas have been synthesized and used on an industrial scale. Some of them, for example fluoro-taeniolite and fluoro-tetrasilicic-mica, are swollen with water into a manner similar to smectites, having interlayer charge densities higher than that of smectites. Unlike natural clays, these have high crystallinity, controllable composition and less impurities. Therefore, use of such micas as host materials is expected to be more advantageous than the use of natural clays. However, there have been few studies on the intercalation chemistry of synthetic fluoromicas.

In the present study, quarternary ammonium (n-alkyltrimethylammonium chlorides, TMA) with a variable chain length are intercalated into synthetic fluorotaeniolite and hectorite. To observe the intercalation process, the intercalation experiments are performed with a controlled exchange ratio. The structures of the organo-mica complexes and the intercalation process are discussed according to the basis of XRD observations.

EXPERIMENTAL

Sample Preparation

The synthetic micas used are commercial fluorotaeniolite (Li-FTN) with the ideal formula of $Li^+(Mg_2Li)Si_4O_{10}F_2$ and fluoro-hectorite (Li-FHT) with the ideal formula of $Li^+_{0.33}(Mg_{2.67}Li_{0.33})Si_4O_{10}F_2$ (Topy Industries Co., Ltd.). The cation exchange capacities (CEC) of the Li-FTN is 215 meq/100 g and the Li-FHT is 58 meq/100 g (Analysis by Ca adsorption method, Topy Industries Co., Ltd). The TMA used for the cation exchange reaction had the formula $[CH_3(CH_2)_{n-1}N(CH_3)_3]^+Cl^-$, n = 4, 8, 12, 16, 18, 22 (NOF Co., Ltd.). A fine powder of the fluoro-micas was stirred with an aqueous solution of the respective ammonium chloride at 60 °C for 6 h. In order to control the exchange ratio, the concentration of TMA was varied at 0.5, 1.0 and 2.0 times the TMA^+/Li^+ ratio, that is, the TMA concentrations are half of, equal to and 2 times the CEC of micas. The solid phase was separated from the suspension by centrifugation at 15,000 rpm for 10 min. Free trimethylammonium ions were removed by washing with dionized water 3

Copyright © 1996, The Clay Minerals Society

https://doi.org/10.1346/CCMN.1996.0440408 Published online by Cambridge University Press

Table 1. Exchange ratio of n-alkyltrimethylammonium (TMA).

Host material	Carbon no.	Exchange ratio§ [TMA]$^+$/Li-$^+$ ratio in suspension‡ 0.5	1.0	2.0
LiFTN†	C-4			0.45
	C-8	0.57	0.62	0.63
	C-12	0.36	0.57	0.64
	C-16	0.49	0.63	0.72
	C-18	0.34	0.43	0.64
	C-22	0.52	0.63	0.60
Li-FHT†	C-4			0.27
	C-8	0.30	0.35	0.36
	C-12	0.32	0.35	0.38
	C-16	0.41	0.41	0.42
	C-18	0.37	0.41	0.49
	C-22	0.34	0.43	0.39

† Measured CEC by Ca adsorption method; Li-FTN: 215 meq/100 g, Li-FHT: 58 meq/100 g.

‡ Starting [TMA]$^+$/Li$^+$ ratio in the [TMA/layer silicate/water] suspension; ratio of added TMA ion per exchangeable Li$^+$.

§ Obtained by TGA measurements from 150 °C to 1000 °C.

times. Finally the solid phase was lyophilized under vacuum ($<10^{-2}$ torr).

Thermogravimetry (TGA)

Thermogravimetric measurements were carried out in the range 30 °C to 1000 °C in air (TAS-200, RIGAKU). The weight of TMA intercalated into mica was estimated from the total weight loss by TGA within the range from approximately 150 to 1000 °C. Samples (approximately 7 mg) were loaded into Pt crucibles in a dry atmosphere and the sample chamber was heated at 10 °C/min in air.

X-ray Powder Diffraction (XRD)

The XRD data of the samples were collected between 1.5 and 65 °2θ at a scanning speed of 1.0 °/min using a powder X-ray diffractometer with Ni-filtered Cu-Kα radiation (RINT 2000, RIGAKU). The relative humidity was fixed at 10% and temperature at 30 °C.

RESULTS

All TMA having different alkylchain lengths formed intercalation complexes with Li-FTN and Li-FHT by a cation exchange reaction between TMA$^+$ and Li$^+$. The exchange ratio was calculated from the amounts of intercalated TMA$^+$, obtained by TGA data and the amounts of exchangable Li$^+$ in fluoro micas (CEC). These data are summarized in Table 1. The exchange ratios ranged from approximately 0.3 to 0.7. Although the intercalation experiments were performed carefully under mild conditions, as suggested by Walker (1967), the exchange ratios between Li$^+$ and TMA$^+$ were somewhat scattered for the different combinations of TMA and mica samples.

XRD Observation

XRD data of the intercalation products show that their basal spacings are expanded to much longer than 9.6 Å, the basal spacing of anhydrous Li-FTN and Li-FHT, indicating that TMAs intercalate into the micas. The XRD patterns of intercalation complexes of Li-FTN and Li-FHT with TMAs of different alkylchain lengths are essentially all similar to each other except for their interlayer distances. Typical XRD patterns are presented for the Li-FTN/docosyl trimethylammonium (C-22) complexes (Figure 1a) and for Li-FHT/octadecyl trimethylammonium (C-18) complexes (Figure 1b). The XRD patterns of the samples treated with different TMA concentrations of 0.5 times the TMA$^+$/Li$^+$ ratio is noted as curve 1, 1.0 times the TMA$^+$/Li$^+$ ratio is noted as curve 2 and 2.0 times the TMA$^+$/Li$^+$ ratio is noted as curve 3 in Figure 1.

The three XRD patterns of the complexes seem to differ significantly from each other despite their compositional similarity (Figure 1a and 1b). XRD peaks observed in Figure 1a are at 39.8 Å, 30.9 Å, 20.0 Å, 15.5 Å and 13.4 Å. The reflections at 20 Å, correspond to the (002) of the peak at 39.8 Å and 15.5 Å corresponds to the (002) of 31 Å. The others cannot be easily assigned. Moreover, some other TMA$^+$/FTN complexes with TMA$^+$ of n = 16, 12 and 8 showed weak XRD peaks at extremely large spacing. Their profiles and dependence on the exchange ratio of TMA$^+$/Li$^+$ are similar to those at 53 Å (Figure 1b).

For understanding the interrelations between the complicated XRD patterns, there are some suggestive behavior in the XRD patterns as the TMA$^+$ concentration varies. The peaks in curve 1 are broader than those in curve 3. The full width at half maximum intensity (FWHM) of the former peak is about one and a half times greater than that of the latter. Curve 2 appears to be intermediate between curve 1 and curve 3, showing the progress of the intercalation reaction.

All spacings observed for the TMA$^+$/FTN (Figure 2a) and TMA$^+$/FHT (Figure 2b) complexes are plotted against the carbon number of the alkylchain. Solid symbols indicate the largest spacings of XRD peaks observed for the samples treated with excess TMA (TMA$^+$/Li$^+$ = 2.0). Examples of these can be seen for the main peaks at 39.8 Å (Figure 1a curve 3) and at 36 Å (Figure 1b curve 3). Open symbols indicate all other spacings observed. They are calculated from 2θ at half-width of each reflection. For both complexes, there are three linear relations between the basal spacings and carbon number within the range of C = 8 to 22 (Figures 2a and 2b). The minimum d-spacing for both complexes at about 13 Å does not change with the carbon number (line *M*). The extremely long spacings appearing for the complexes treated with lower concentrations of TMA form a linear row with an in-

https://doi.org/10.1346/CCMN.1996.0440408 Published online by Cambridge University Press

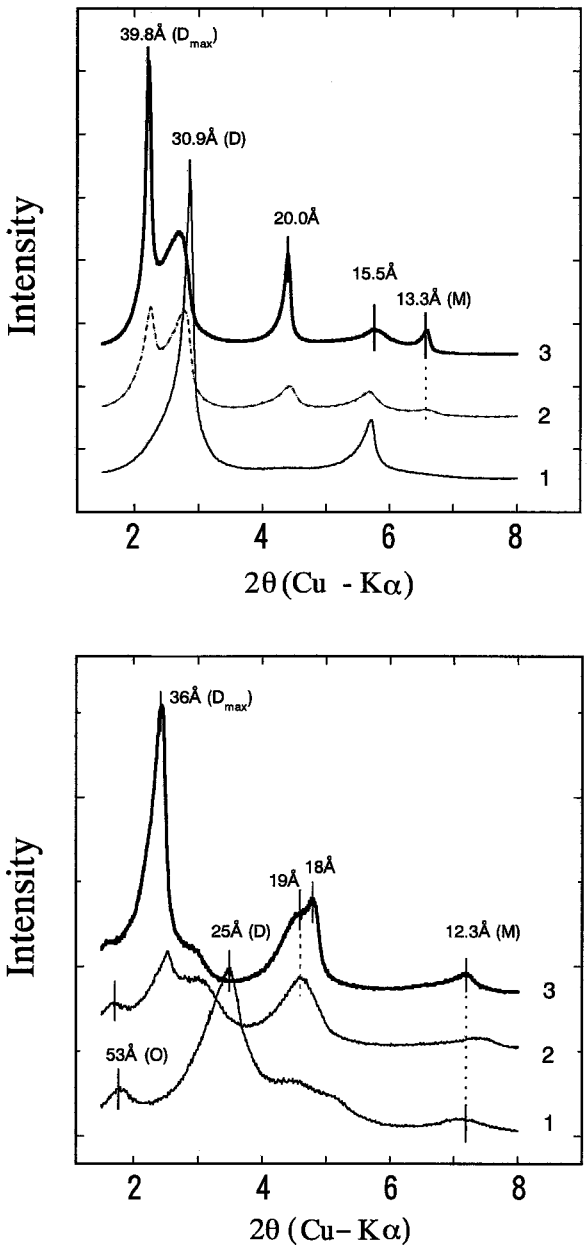

Figure 1. XRD patterns of mica/TMA complexes: a) Li-FTN/C-22 TMA complexes; and b) Li-FHT/C-18 TMA complexes. The patterns are displaced vertically with added organic content from bottom to top as follows: 0.5 $[TMA]^+/Li^+$ ratio corresponds to curve 1, 1.0 $[TMA]^+/Li^+$ ratio corresponds to curve 2 and 2.0 $[TMA]^+/Li^+$ ratio corresponds to curve 3.

crease of the TMA carbon number (line *O*). The rows of solid symbols, which are the d-spacings of the main reflections, also have linear dependence upon the carbon number (line D_{max}). The variations of the interlayer spacing shown by the lines clearly indicate the state of intercalation and the process involved.

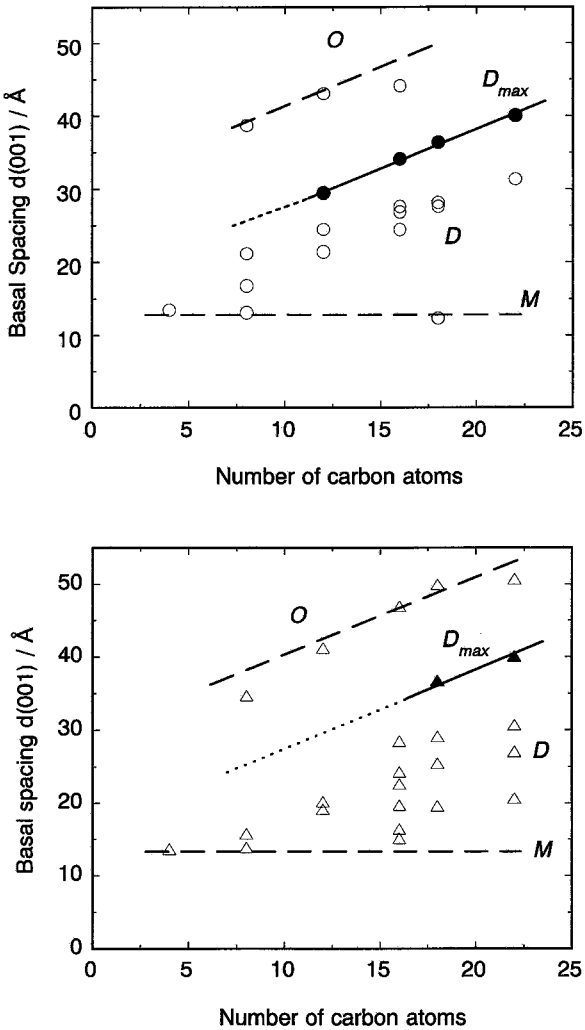

Figure 2. d(001) spacings observed for a) Li-FTN complexes; and b) Li-FHT complexes. Key: Solid symbols = main reflection appeared at the mature stage of intercalation. Open circles = all other peaks appeared.

DISCUSSION

The XRD patterns (Figure 1) of the TMA intercalation phenomena of synthetic fluoro micas are similar to, but much clearer than those of natural clays. The micas and TMA formed several complexes of different interstratification depending upon maturity of the intercalation reaction. The identification of the phases that appeared and the intercalation mechanism will be discussed.

The Observed Phases: Regularly and Randomly Interstratified Organo/Fluoro Mica Complexes

Four phases were identified for the intercalation complexes by interpreting the XRD patterns described previously. They are called for D_{max}, *D*, *O* and *M* phases. Phase D_{max} is the main phase of the complexes

https://doi.org/10.1346/CCMN.1996.0440408 Published online by Cambridge University Press

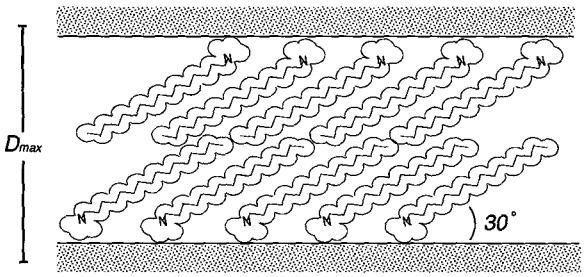

Figure 3. Paraffin-type bilayer model of mica/C-18 ammonium complexes.

formed by the treatment at the highest TMA^+ concentration of 2.0. The XRD peak intensities of the other phases all decreased with increasing TMA^+ concentration (Figure 1a and 1b). The D_{max} phase is the final state of the intercalation, whereas the other phases are stable only at the initial or intermediate stages of intercalation. The phase *M* is not a phase of the organo/mica complex but corresponds to hydrated mica, which was deduced from its d-spacing of approximately 13 Å independent of the variable chain length of TMA treated. The *O* phase is a phase stable only during the intermediate stage of intercalation reaction and has an interlayer spacing equal to the sum of those of the D_{max} and *M* phases, indicating the regular interstratification of the two unit layers. The *D* phase is interpreted as having random stratification of unit layers of the phases D_{max} and *M*. The continuously variable d-spacings of the *D* phase are due to variation of the number of the layers intercalated by TMA^+.

FHT and FTN exhibit quite similar intercalation behavior. However, the intercalation of FHT is more sluggish and heterogeneous than that of FTN, which is similar to that of natural clay. This is deduced from the observations that: 1) the *O* phase appears often with treatment at the highest TMA^+ concentration of 2.0; and 2) the XRD peaks of the TMA/FHT composites are broader than those of Li-FTN, especially for those treated at a low TMA^+/Li^+ ratio (Figures 1a and 1b). Moreover, the TMA/FHT complexes showed many more *D* phase peaks in the XRD pattern than do the TMA/FTN complexes (Figures 2a and 2b). These differences for the intercalation behaviors of Li-FTN and Li-FHT are probably due to the differences between crystallinity and homogeneity of charge distribution of the host materials.

Alkylchain Arrangements of the Mica Interlayers

Alkylchain arrangements of the mica interlayers are reasonably modeled for the D_{max} phase using the observed d-spacings and some simple assumptions that the alkylchain is part of the straight form and has minimum contact with neighboring molecules, such as a paraffin-type bilayer structure with long chains inclined at about 30° to the silicate sheet. The model for the C-18 TMA/mica complex is shown in Figure 3. The angle of chain inclination is calculated from the slope of the d-spacing vs. alkylchain carbon number (Figures 2a and 2b). This is the final structure of TMA intercalation reaction into micas. The Li-FTN forms this structure between the range of carbon number from C-12 to C-22 and Li-FHT between the range from C-18 to C-22. The *O* phase and the *D* phase are regularly and randomly interstratified structures of unit layers of the *M* and the D_{max} phases. The *M* phase is the hydrated mica having a layer of water molecules within the interlayer, and is empty for TMA. The models explain the linear dependency of the d-values upon the carbon number of TMA and the intercalation process.

The Intercalation Process of TMA Into Micas

The XRD patterns of the intercalation complexes showed obvious change depending upon the TMA^+/Li^+ ratio treated (Figures 1a and 1b). The change in those patterns shows the intercalation process of TMA into micas, which may be explained visually by using the intercalation models noted previously.

The *O* and the *D* phases are dominant at the intermediate stage of the intercalation reaction, and the D_{max} phase appears finally as the stable state. This indicates that TMA intercalates into the mica interlayer as a unit layer of the D_{max} structure (Figure 3). The layers interstratify with the empty unit layers of the *M* phase partially regularly (the *O* phase) and partially randomly, adjusting the composition of the complex to that of the TMA^+/Li^+ ratio (the *D* phase). As the number of TMA-intercalated layers is increased, the *D* phase converts gradually to the D_{max} phase and the *M* or *O* phase disappears.

Comparison with Previous Models

A previous study on n-alkylammonium intercalation to vermiculites concluded that alkylchains oriented at 55° ± 5° to the silicate sheet within the interlayer and the variable interlayer spacing observed was attributed to some artifacts introduced during the washing and drying process (Johns and Sen Gupta 1967). Conversely a recent study by Fourier transform infrared spectroscopy (FTIR) of the alkyl chains intercalated into montmorillonite and fluoro-hectorite indicated that the chains are flexible and assume solid, liquid or liquid-crystal states depending upon the interlayer packing density, temperature and chain length (Vaia et al. 1994). These studies may be helpful for interpretation of variable XRD patterns. However, there has been no consideration of the intercalation process during previous studies. In the present study, the variable XRD peaks observed have been reasonably interpreted as the phases appearing during the maturation process of the intercalation reaction. The regularly and ran-

https://doi.org/10.1346/CCMN.1996.0440408 Published online by Cambridge University Press

domly interstratified structures found during the present work are key structures to explain the intercalation mechanism of TMA into micas and the variety of XRD patterns of the complexes.

CONCLUSION

Li-FTN and Li-FHT form intercalation complexes with TMA having different chain lengths. With an increasing exchange ratio of TMA^+/Li^+, the complexes initially take regularly and randomly interstratified structures with layer units of TMA and water intercalated layers. Finally, the complexes take a "paraffin-type bilayer structure", where the long chain of TMA inclines at about 30° to the silicate sheet. Li-FHT and Li-FTN showed quite similar intercalation characteristics, but Li-FTN is the better host. This was demonstrated by the narrower FWHM of the (001) reflections and by the sharper transition from the regularly and randomly interstratified complexes to the final structure. The difference can predominantly be attributed to higher layer charge and crystallinity of Li-FTN.

ACKNOWLEDGMENTS

The authors are grateful to T. Fujita, N.I.R.I.M., for his experimental support throughout this work and to J.R. Hester, N.I.R.I.M., for his english corrections. We thank also H. Inoue. Showa Denko K.K., for his help in $C_4H_9N^+(CH_3)_3$ Cl^-, $C_8H_{17}N^+(CH_3)_3Cl^-$ sample preparation, and A. Ando, Topy Industries Co., Ltd., for supplying Li-FTN and Li-FHT samples.

REFERENCES

Farmar VC, Mortland MM. 1965. An infrared study of complexes of ethylamine with ethylammonium and copper ions in montmorillonite. J Phys Chem 69:683–686.

Fukushima Y, Inagaki S. 1987. Synthesis of an intercalated compound of montmorillonite and 6-polyamide. J Incl Phenom 5:473–482.

Lagaly G, Weiss A. 1969. Determination of the layer charge in mica-type layer silicates. In: Heller L, editor. Proceedings of the International Clay Conference, Tokyo, Japan. p 61–80.

Johns WD, Sen Gupta PK. 1967. Vermiculite-alkyl ammonium complexes. Am Mineral 52:1706–1724.

MacEwan DMC, Wilson MJ. 1980. Interlayer and intercalation complexes of clay minerals. In: Brindley GW, Brown G, editors. Crystal structure of clay minerals and their X-ray identification. London: Mineralogical Society. p 197–248.

Magaruran ED, Kieke MD, Reichert WW, Chiavoni A. 1987. Effective vitilization of organoclay dispersants. NGLI Spokesman 50:453–460.

Messersmith PB, Giannelis EP. 1994. Synthesis and characterization of layered silicate-epoxy nanocomposites. Chem Mater 6:1719–1725.

Vaia RV, Rachel KT, Giannelis EP. 1994. Interlayer structure and molecular environment of alkylammonium layered silicates. Chem Mater 6:1017–1022.

Walker GF. 1967. Interactions of n-alkylammonium ions with mica-type layer lattices. Clay Miner 7:129–143.

Wang MS, Pinnavaia TJ. 1994. Clay-polymer nanocomposites formed from acidic derivatives of montmorillonite and an epoxy resin. Chem Mater 6:468–474.

Yan Y, Bein T. 1993. Molecular recognition through intercalation chemistry: Immobilization of organoclays on piezoelectric devices. Chem Mater 5:905–907.

(Received 30 May 1995; accepted 29 October 1995; Ms. 2655)

https://doi.org/10.1346/CCMN.1996.0440408 Published online by Cambridge University Press